Conformational analysis of α-D-Fuc-(1→4)-β-D-GlcNAc-OMe. One-dimensional transient NOE experiments and Metropolis Monte Carlo simulations

Thomas Weimar[a], Bernd Meyer[b] and Thomas Peters[a,*]

[a]*Institute for Biophysical Chemistry, University of Frankfurt, Theodor-Stern-Kai 7-15, Bldg. 75A, 6000 Frankfurt 70, Germany*
[b]*Complex Carbohydrate Research Center and Department of Biochemistry, The University of Georgia, Athens, GA 30602, U.S.A.*

SUMMARY

One-dimensional transient NOE build-up curves were measured for the synthetic disaccharide α-D-Fuc-(1→4)-β-D-GlcNAc 1 utilizing Gaussian shaped pulses. Simulated build-up curves from Metropolis Monte Carlo simulations were compared to the experimental data. Disaccharide 1 is structurally related to methyl β-D-maltoside in that it also contains an α-(1→4) linkage, and it has the same configuration of groups around the glycosidic linkage. Analysis of NOEs in methyl β-D-maltoside is restricted to those observed upon selective excitation of H1′ because of severe spectral overlap. The situation is different in 1 where ¹H-NMR signals are well separated. Several interglycosidic NOEs were observed. The corresponding build-up curves allowed an accurate determination of the conformational preferences at the glycosidic linkage in 1. Comparison of experimental and theoretical NOE build-up curves showed clearly that rigid minimum-energy models cannot account for the experimental data. The best fit of experimental NOE build-up curves was obtained with theoretical curves from a 2×10^6 step Metropolis Monte Carlo simulation with the temperature parameter set at 1000 K. Finally, it was observed that only the interglycosidic NOE H5′/H6-*pro*-S significantly depends upon varying conformation distributions at the α-(1→4)-glycosidic linkage, induced by choosing different temperature parameters for the Metropolis Monte Carlo simulations.

INTRODUCTION

Conformational analysis of carbohydrates relies to a great extent on the observation of interglycosidic NOEs (Bock, 1983; Meyer, 1990). These effects are often sparse and much of the data published so far is of low accuracy biasing a quantitative treatment. The introduction of hydroxyl

---

*To whom correspondence should be addressed.

protons as long-range NOE sensors (Poppe and van Halbeek, 1991a) and of pulse sequences to accurately measure heteronuclear (^{13}C,^{1}H) vicinal coupling constants (Poppe and van Halbeek, 1991b) extends the range of conformation-dependent parameters that can be determined, but still, the problem of low-accuracy NOE data remains. It is widely recognized now that saccharides cannot be treated as rigid molecules but display considerable flexibility (Cumming and Carver, 1987a,b; Imberty et al., 1989; Bock et al., 1990; Homans, 1990; Peters et al., 1990; Poppe et al., 1992; Widmalm et al., 1992; Peters et al., 1993), especially around glycosidic linkages and side chains. Therefore, theoretical calculations of NMR parameters must take into account that these data represent ensemble average values. We use a Metropolis Monte Carlo (MMC) simulation method (Peters et al., 1993) implemented in the program GEGOP (Stuike-Prill and Meyer, 1990) to predict such ensemble average values.

To our knowledge there have been no attempts yet to analyze the conformational properties of small saccharides on the basis of NOE build-up curves from 1D transient NOE experiments in combination with a subsequent comparison to theoretical ensemble-averaged build-up curves. Earlier work mostly used steady-state NOE experiments (Noggle and Schirmer, 1971) and several more recent studies employed 2D or 1D NOESY experiments (Marion and Wüthrich, 1983; Kessler et al., 1986). For small NOEs 1D transient NOE experiments are preferable over steady-state or 1D/2D NOESY experiments because maximum transient NOE enhancements are significantly larger (Neuhaus and Williamson, 1989). This is especially important in quantitative data analysis. Compared to NOESY enhancements there is a theoretical factor of two in intensity, everything else being equal. For an ideal two-spin system the theoretical maximum steady-state enhancement is 50% compared to 38.5% for the maximum transient enhancement, but in practice the reversed order is observed, presumably because the faster initial growth in transient experiments more effectively competes with external relaxation (Williamson and Neuhaus, 1987). Recently, the calculation of ensemble average build-up curves from MD simulations was reported for the disaccharide α-L-Rha-(1 $\rightarrow$ 2)-α-L-Rha-OMe (Widmalm et al., 1992). The latter study was based upon 2D NOESY build-up curves obtained in DMSO-D$_2$O at $-30°$C. These 'unphysiological' conditions were chosen because 2D NOEs were too weak at room temperature.

Here, we present experimental 1D transient NOE build-up curves at room temperature for the synthetic disaccharide α-D-Fuc-(1 $\rightarrow$ 4)-β-D-GlcNAc-OMe 1. Theoretical ensemble average NOE build-up curves were obtained from MMC simulations and compared to experimental data. Disaccharide 1 is related to maltose that has been the subject of a number of conformational analyses in the past (Lemieux and Bock, 1983; Lipkind et al., 1985; Pérez and Vergelati, 1987; Ha et al., 1988; French, 1989; Tran et al., 1989; Peters et al., 1993). In maltose there is severe overlap of ^{1}H NMR signals prohibiting selective excitation of protons other than the anomeric protons. The situation is different in 1 where spectral dispersion of ^{1}H NMR signals is greatly improved (Fig. 1a).

EXPERIMENTAL

α-D-Fuc(1 $\rightarrow$ 4)-β-D-GlcNAc-OMe 1 was synthesized (T. Weimar and T. Peters, unpublished results) according to the protocol published before (Peters and Weimar, 1991) with a D- instead of the L-fucopyranosyl glycosyl donor (Dejter-Juszynski and Flowers, 1971) derived from D-galactopyranose. After exchanging hydroxyl protons against deuterium atoms an NMR sample
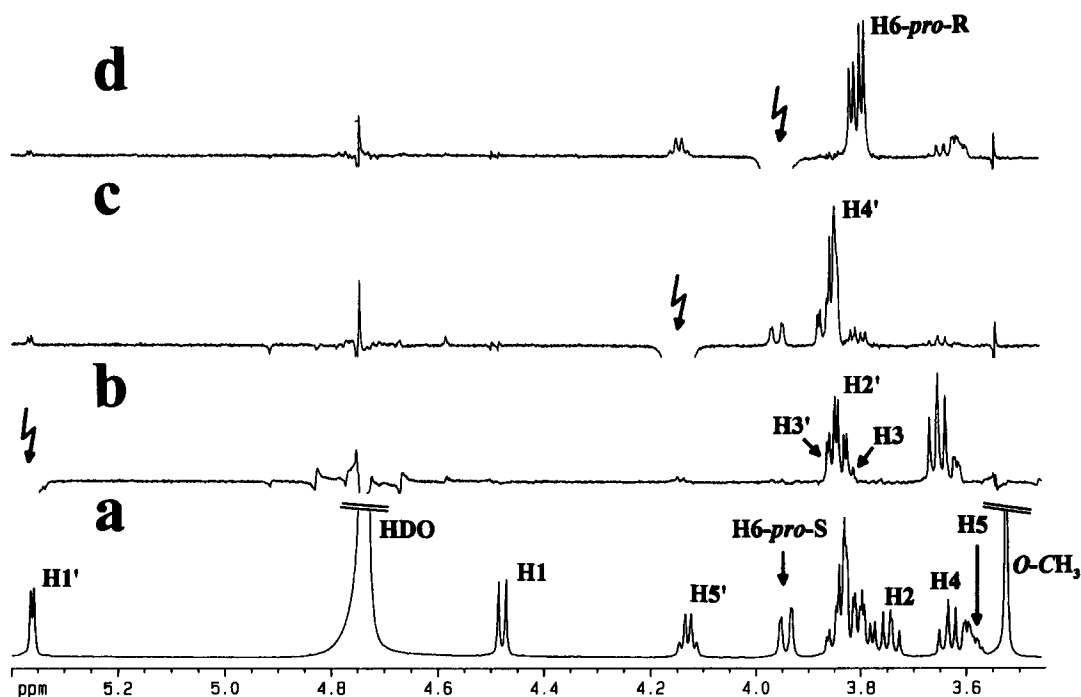
Fig. 1. 1D transient NOE difference spectra of 1 in D_2O at 303 K. The mixing time was 940 ms in all cases. A Gaussian-shaped 180° pulse of 80 ms was used to selectively excite the proton resonances. Traces (b)–(d): selective excitation of H1', H5' and H6-*pro*-S. For each spectrum, 256 scans were recorded. As a reference trace (a) shows the ^{1}H NMR spectrum of 1.

was prepared by dissolving 10 mg of 1 in 0.5 ml of D_2O (99.996%, MSD Isotopes) resulting in a 52-mM solution. Oxygen was removed from the sample by repeated evacuation from an argon atmosphere. Finally, the sample was sealed under argon.

NMR experiments were performed on Bruker AM 500 and AMX 600 spectrometers operating at proton frequencies of 500.13 and 600.14 MHz, respectively. All measurements were performed at 303 K using the HDO signal as internal standard (4.722 ppm at 303 K). All spectra were acquired with a spectral width of 6 ppm. Nonselective T_1 values were determined at 500 MHz using the nonselective inversion-recovery technique (Vold et al., 1968). 1D transient NOE experiments (Heatley et al., 1980) were performed at 600 MHz with 256 scans each. Subtraction of on-and off-resonance spectra was achieved via phase cycling. Gaussian-shaped 180° pulses (80 ms) were used for selective excitation (Kessler et al., 1986). Calibration of Gaussian pulses was performed according to the literature (Kessler et al., 1986; Anders, 1989). Half of the pulse duration (40 ms) was added to the mixing times used giving corrected mixing times of 41, 115, 190, 380, 640, 940 and 1240 ms. FIDs were recorded with 8K data points and zero-filled prior to Fourier transformation to give spectra with 16K data points. A relaxation delay of 3 s was used.

Prior to integration of NOEs a third-order baseline correction was performed on a Bruker X32 workstation. In cases where NOEs of overlapping signals had to be determined a line deconvolu-

tion was performed, using Bruker standard software. The decay curves of selectively excited signals were used to scale the NOE build-up curves. It was assumed that the decay curves followed an exponential function of the form $f(\tau_m) = C \exp(-\tau_m/T_{1sel})$ in all cases, with C = scaling factor, τ_m = mixing time and T_{1sel} = selective spin-lattice relaxation time. Experimental decay curves were fitted to this exponential function using a FORTRAN program which employed a nonlinear least-squares fitting procedure according to the Levenberg-Marquardt algorithm (Press et al., 1986). This fitting process also gives experimental T_{1sel} values.

To assess the experimental error, the overall shape of build-up curves was taken as an estimate. Most of the build-up curves are rather smooth indicating a small experimental error.

MMC simulations (Peters et al., 1993) and calculation of global and local minima of 1 were performed with the program GEGOP (Stuike-Prill and Meyer, 1990) employing a modified (Poppe et al., 1992) HSEA (Thøgersen et al., 1982) force field. Coordinates for β-D-N-acetyl glucosamine and for α-L-fucose were obtained from X-ray diffraction data (Cook and Bugg, 1975; Winter et al., 1978). α-D-Fucose coordinates were generated by mirror-imaging α-L-fucose coordinates. Hydrogen atoms were deleted and replaced with standard geometries. Pyranose rings were treated as rigid, leaving the dihedral angles φ and ψ and the bond angles τ at the glycosidic linkages as the only variables. At glycosidic linkages, dihedral angles φ, ψ and ω and bond angles τ were defined as follows: φ = H1–C1–O1–CX, ψ = C1–O1–CX–HX, ω = O5–C5–C6–O6 and τ = C1–O1–CX with X being the aglyconic linkage site. The bond angle τ was optimized with a harmonic spring potential with an equilibrium τ value of 117°. For the MMC simulations all exocyclic dihedral angles and glycosidic bond angles τ were treated as flexible with maximum step lengths set at 20° (303 K) or 40° (1000 K) for φ and ψ, at 25° (303 K) or 45° (1000 K) for ω, and at 2.5° (303 K, 1000 K) for τ. MMC simulations were carried out on a Silicon Graphics IRIS 4D/35 workstation or on a Convex C1 with 2×10^6 macro steps each and temperature parameters set at 303 K and 1000 K. The overall acceptance ratios were 43% (303 K) and 45% (1000 K). Another set of 10^5 macro-step MMC simulations with temperature parameters again set at 303 and 1000 K was performed with ω (maximum step length = 25° (303 K, 1000 K)) being the only variable parameter and the residual angles set at values found for minima A–D (Fig. 1).

NOEs were calculated assuming isotropic molecular motion and neglecting effects from strong scalar coupling (Kay et al., 1986) and cross-correlation (Bull, 1987; Krishnan and Kumar, 1991) by solving Eq. 1 (Boelens et al., 1989; Borgias and James, 1989). 5% solvent relaxation was assumed. Elements of the relaxation matrix R were calculated in the same way as has been explained in detail earlier (Brisson and Carver, 1983; Peters et al., 1990,1993). It should be emphasized that off-diagonal elements of R are twice as large as in the case of 1D/2D NOESY experiments. Equation 1 was solved numerically as Eq. 2:

$$A(\tau_m) = \exp[-R\,\tau_m] \tag{1}$$

$$A(\tau_m) = X \exp[-\lambda\,\tau_m]\,X^{-1} \tag{2}$$

with A = NOE matrix, R = relaxation matrix, λ = diagonal Eigenvalue matrix obtained by diagonalization of R ($\lambda = X^{-1} R X$), X = matrix of Eigenvectors of R and τ_m = mixing time as used in the experiments. Diagonalization was performed by linking routines from the LAPACK library

(University of Tennessee, University of California Berkeley, NAG Ltd., Courant Institute, Argonne National Lab. and Rice University, 1992) to GEGOP. The relaxation matrix $\mathbf{R}$ was obtained either via proton-proton distances r for one of the low-energy conformers A–D or via average $<r^{-3}>$ values from MMC simulations as has been explained in detail before (Peters et al., 1993). NOEs from MMC simulations were denoted as $<NOE>_{MMC}$.

The overall motional correlation time τ_c was estimated by fitting an MMC simulated ensemble-average decay curve of a selectively excited proton signal to the corresponding experimental curve. The NOE experiments with selective inversion of protons H1' and H5' were chosen for this purpose. τ_c was varied in a range of 0.1–0.4 ns and standard deviations were calculated for the deviation of theoretical curves (obtained from Eqs. 1 and 2) from experimental curves. For $\tau_c = 0.2$ ns standard deviations were at a minimum, which is in accordance with data obtained earlier from ^{13}C T_1 data for similar disaccharides (Brisson and Carver, 1983; Peters et al., 1990). This value was used to calculate NOEs. Methyl groups undergo fast internal rotation and require a special treatment (Heatley et al., 1980; Brisson and Carver, 1983). The protocol applied here to the methyl groups is based on expressions given by Rowan and Sykes (1975) assuming an internal correlation time (Brisson and Carver, 1983) τ_i of 10^{-13} s.

Experimental vicinal homonuclear coupling constants $J_{5,6}$ were used to calculate the populations of gt, gg and tg rotamers in **1** using the Karplus equation as parametrized by Haasnoot et al. (1980), by Streefkerk et al. (1973) and by Gerlt and Youngblood (1980).

Graphical presentation of the potential-energy surface of **1** was achieved with the program SURFER (Golden Software) running on IBM PCs or compatibles. MMC trajectories were plotted with FORTRAN software using the NCAR library (NCAR Graphics, Version 3.0, December 1989, Scientific Computing Division, National Center of Atmospheric Research, Boulder, Colorado). Population plots at 1° resolution were calculated with the program GPTOOL which is part of the GEGOP (Stuike-Prill and Meyer, 1990) package and plotted and integrated with EXCEL (Microsoft).

RESULTS

NMR experiments

^1H NMR signals of α-D-Fuc-(1→4)-β-D-GlcNAc-OMe **1** were assigned using standard COSY and NOESY experiments (Table 1). Stereospecific assignments of the prochiral protons H6-*pro*-R and H6-*pro*-S are in analogy to D-glucose (Ohrui et al., 1985; Nishida et al., 1988) and vicinal coupling constants $J_{5,6}$ were derived from 1D ^1H NMR spectra or transient NOE experiments. Vicinal coupling constants $^3J_{H,H}$ confirmed that both pyranose rings in **1** adopt the $^4C_1$ conformation. 1D NOESY (Marion and Wüthrich, 1983) and 1D transient NOE experiments were performed to experimentally assess the glycosidic linkage conformation in **1**. It turned out that 1D transient NOE experiments not only had the advantage of a theoretical factor of two for intensity gain but also showed no phase-distortion effects. Phase-distortion effects (Kessler et al., 1991) were observed in 1D NOESY spectra of **1** in case of spin-spin coupled proton pairs biasing their quantitative treatment. In principle a delay [≈ (1/2) − (length of selective pulse/2)] (Anders, 1989) can be included into the 1D NOESY sequence after the selective 90° pulse to eliminate this problem. However, for **1** several coupling constants are small (1–4 Hz) giving rise to rather long delays that in turn cause significant loss of magnetization. Therefore, all build-up curves were

TABLE 1

CHEMICAL-SHIFT VALUES δ, COUPLING CONSTANTS J, NONSELECTIVE (T₁) AND SELECTIVE (T₁ₛₑₗ) RELAXATION TIMES OF 1

Proton	δ [ppm]	J [Hz]	T_1 [s][b]	T_{1sel} [s]
α-D-Fuc				
H1'	5.34	$J_{1,2} = 3.6$	0.9	1.4
H2'	3.81	$J_{1,2} = 3.6^c\ J_{2,3} = 10.4^c$		
H3'	3.84	$J_{2,3} = 10.4^c\ J_{3,4} = 3.1^c$		
H4'	3.82			
H5'	4.12	$J_{5,6} = 6.5$	0.6	1
H6'	1.23	$J_{5,6} = 6.5$	0.6	
β-D-GlcNAc				
H1	4.46	$J_{1,2} = 8.4$	0.9	
H2	3.72	$J_{1,2} = 8.4\ J_{2,3} = 10.3$		
H3	3.8	$J_{2,3} = 10.3^c\ J_{3,4} = 8.3^c$		
H4	3.62	$J_{3,4} = 8.3\ J_{4,5} = 9.8$	0.8	1.2
H5	3.57		0.7	1.2
H6-pro-S	3.93	$J_{5,6proS} = 1.8$	0.4	0.6
		$J_{6proR,6proS} = 12.1$		
H6-pro-R	3.77	$J_{5,6proR} = 5.4^c$		
		$J_{6proS,6proR} = 12.1^c$		
N-Ac	2.03		1	
O-Me	3.51		1	

[a] δ and J values were determined from a first-order analysis. Measurements in D₂O at 600 MHz and 303 K. HDO was used as internal standard (δ = 4.722), referenced against internal acetone (δ = 2.225).

[b] Measured at 500 MHz.

[c] Obtained from 1D transient NOE spectra.

[d] Due to strong coupling, signals cannot be separated.

obtained with 1D transient NOE experiments. 1D transient NOE experiments with a mixing time of 750 ms were performed for all resonance signals sufficiently separated to identify those which were suitable for the measurement of accurate build-up curves and which at the same time provided information about the glycosidic linkage orientation. The signals selected were H1', H5' and H6-pro-S (Fig. 1). In maltose only H1' can be used for a quantitative determination of interglycosidic NOEs. In 1 the following interglycosidic NOEs were found: H1'/H3, H1'/H4(H5), H5'/H4(H5), H5'/H6-pro-R, H5'/H6-pro-S and H6-pro-S/H5'. The notation H4(H5) indicates strong scalar coupling between these two protons. To quantitate the enhancements of the reso-nance signals for H6-pro-R and H3, observed upon selective excitation of H5' and H1', respec-tively, line deconvolutions had to be performed. Transient NOE experiments with selective Gaussian-shaped 180° pulses do not allow spectra to be recorded with infinitely short mixing times as is possible in 1D NOESY experiments (Kessler et al., 1991). Therefore, mixing times and integrals had to be corrected as described in the experimental section. The fitting procedure also yields selective spin-lattice relaxation times T₁ₛₑₗ of the protons selectively excited. In addition, nonselective T₁ values were measured. T₁ₛₑₗ and T₁ values obtained are included in Table 1.
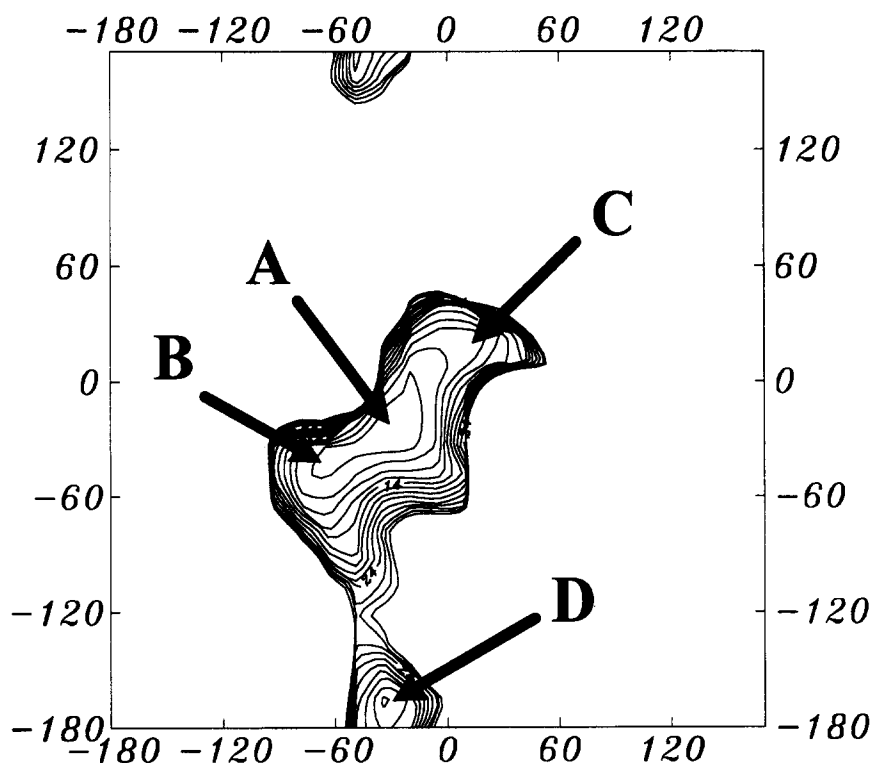
Fig. 2. Contour plot for the energy surface of the α-(1→4)glycosidic linkage in 1 calculated with GEGOP (Stuike-Prill and Meyer, 1990). Four main minima A–D were identified: A, $\phi_{14} = -40°$, $\psi_{14} = -27°$, $E_{rel} = 0.0$ kcal/mol; B, $\phi_{14} = -62°$, $\psi_{14} = -43°$, $E_{rel} = 1.4$ kcal/mol; C, $\phi_{14} = 12°$, $\psi_{14} = 26°$, $E_{rel} = 6.7$ kcal/mol; D, $\phi_{14} = -34°$, $\psi_{14} = -167°$, $E_{rel} = 6.8$ kcal/mol.

Metropolis Monte Carlo simulations

It is known that force-field calculations for maltose yield several local minima indicating that averaging over glycosidic-linkage conformations is necessary to explain experimental NMR data such as NOEs. For 1, four main local minima (A–D, Fig. 2) equivalent to those found in maltose could be identified using the GEGOP program which employs an extended (Poppe et al., 1992; Stuike-Prill and Meyer, 1993) HSEA (Thøgersen et al., 1982) force field. MMC simulations with 2×10^6 macro steps were performed with two different temperature parameters, 303 K and 1000 K. At 303 K the barrier between minima A, B and C on the one hand and minimum D on the other hand was not surmounted but a temperature parameter of 1000 K led to frequent transitions between both regions (Fig. 3). Integration of the respective conformation distributions (Fig. 4) showed that the area around minimum D comprises only 2.5% of all conformational states (compare Lipkind et al., 1985). The rotamer distribution at the C5-C6 bond is slightly changed when increasing the temperature parameter from 303 K to 1000 K. Integration of the rotamer distribution at the C5-C6 bond yields the following rotamer populations: gg (52%), gt (45%), tg (3%) at 303 K, and gg (42%), gt (43%), tg (15%) at 1000 K. Here, gg, gt and tg are defined as the integrated regions ω from 0° to −120°, from 0° to 120° and from 120° to 240°, respectively.

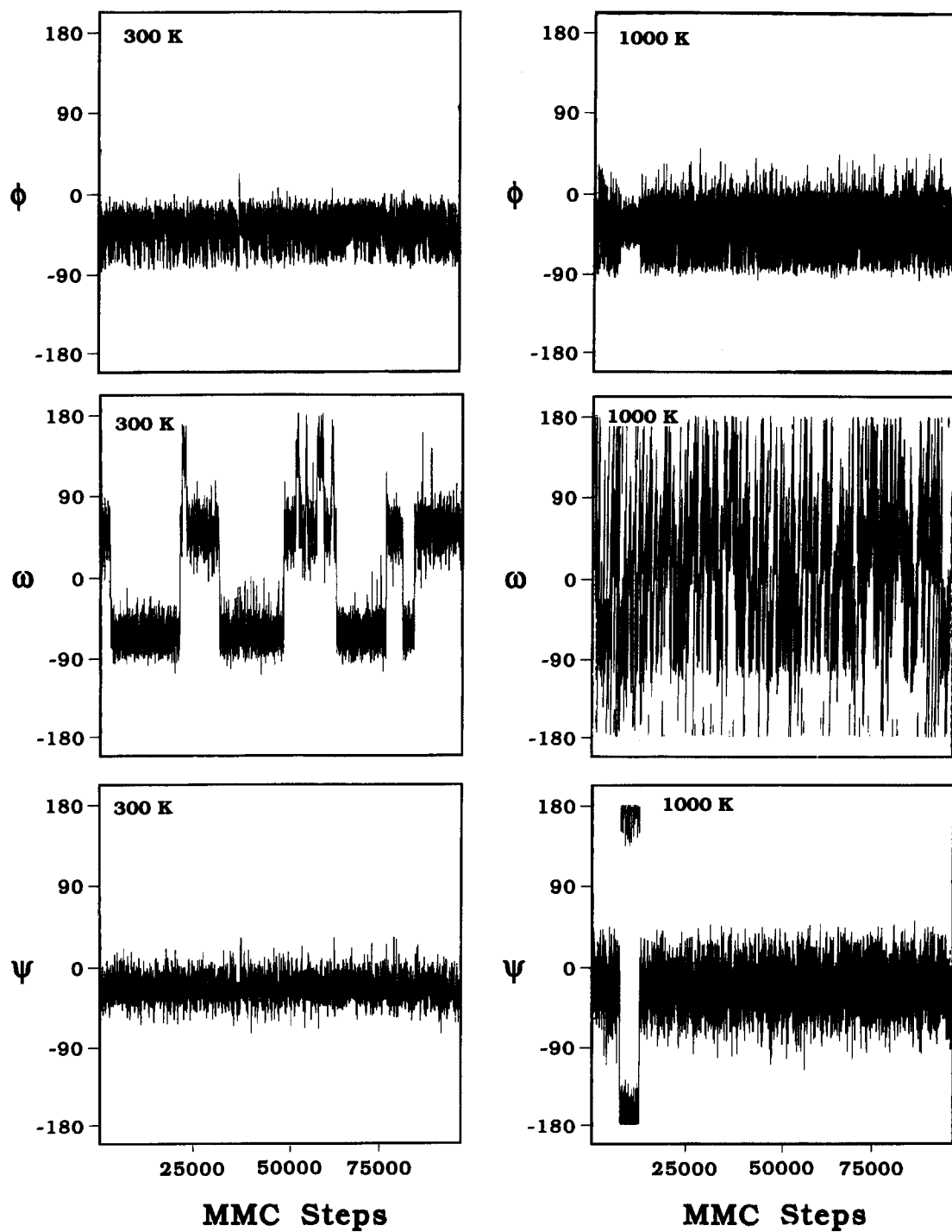For the MMC simulations all exocyclic dihedral angles ϕ, ψ and ω and glycosidic bond angles τ

Fig. 3. Trajectories for the first 10^5 macro steps of the MMC simulations. The dihedral angles ϕ and ψ at the α-$(1 \rightarrow 4)$ glycosidic linkage and ω at the C5-C6 bond in 1, with temperature parameters set at 303 K and 1000 K, are shown as a function of the number of MMC macro steps.
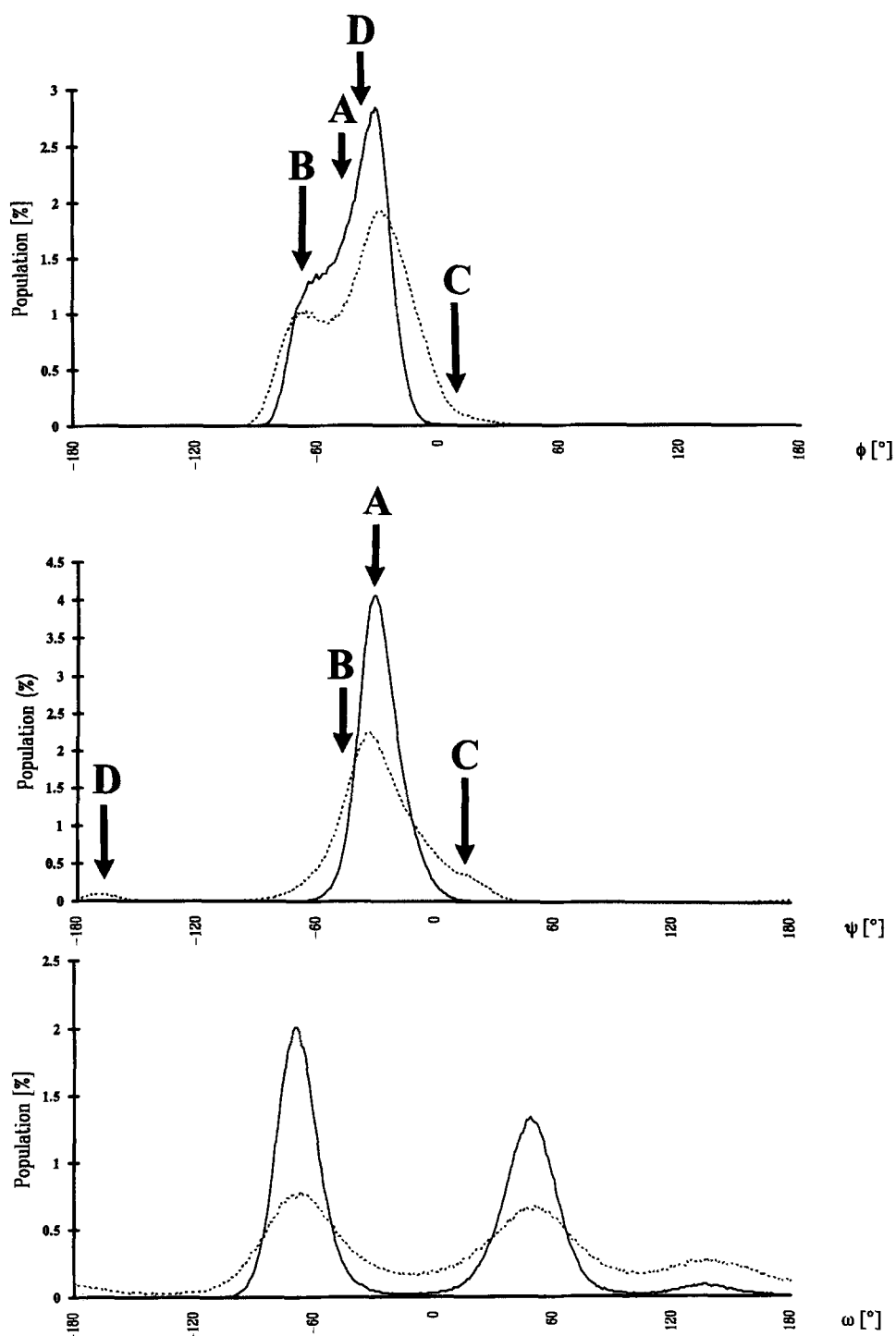
Fig. 4. Population distributions for the dihedral angles ϕ and ψ at the α-(1→4) glycosidic linkage and ω at the C5-C6 bond in **1**. ϕ and ψ coordinates are indicated with arrows. Temperature parameters were 303 K (solid lines) and 1000 K (dotted lines).
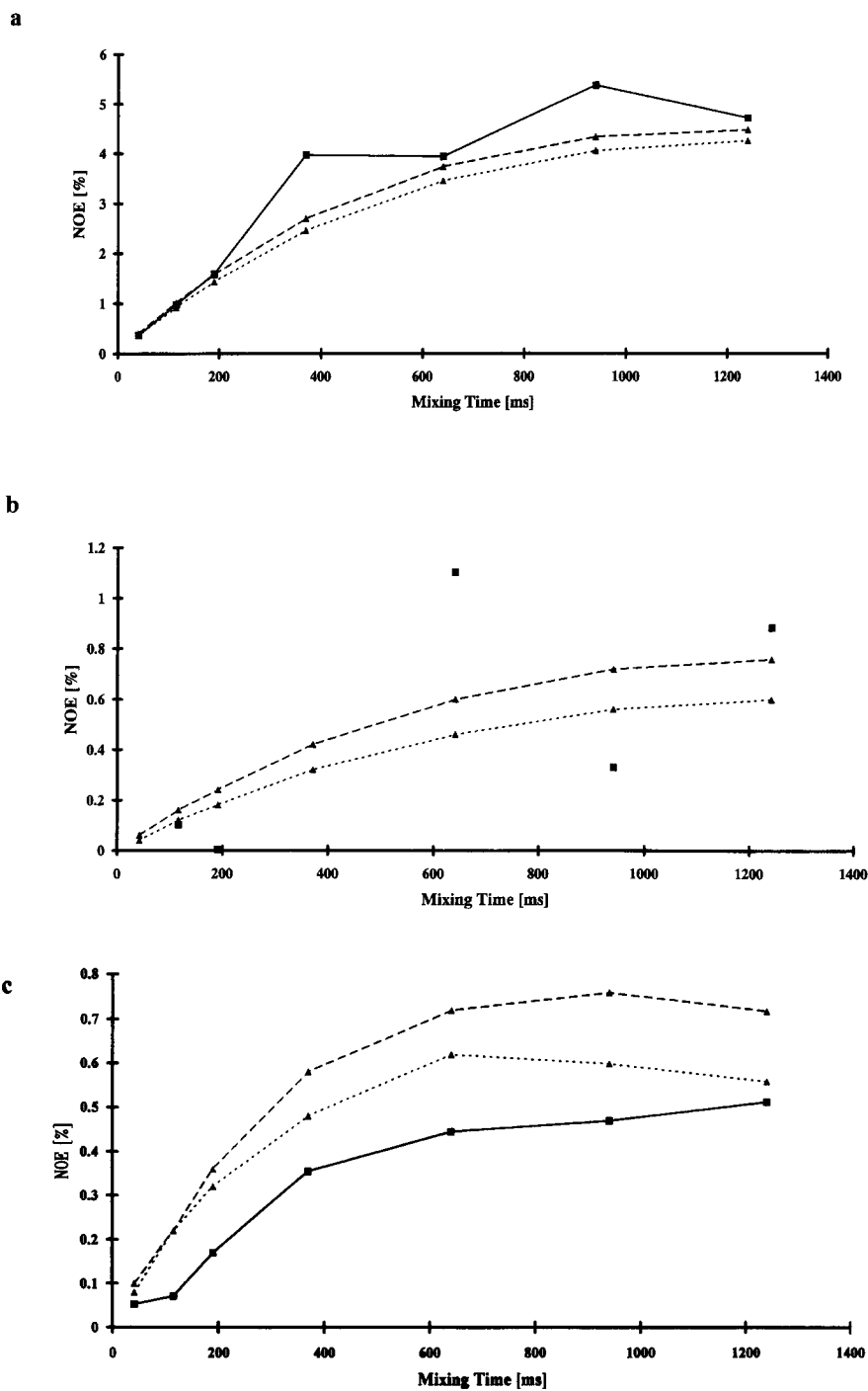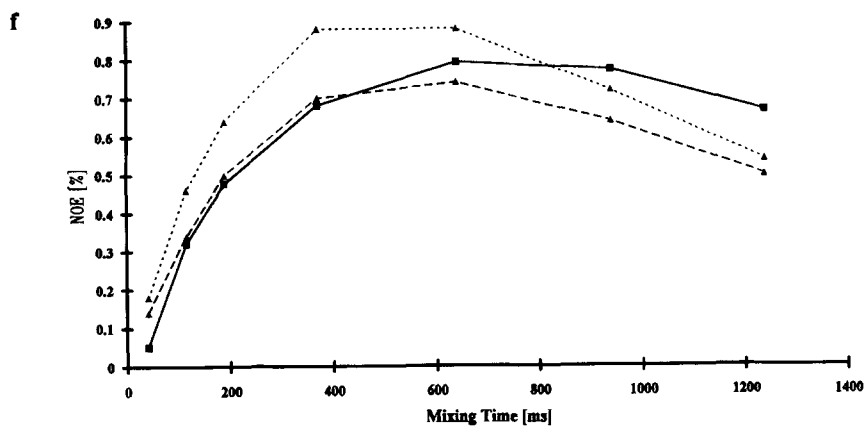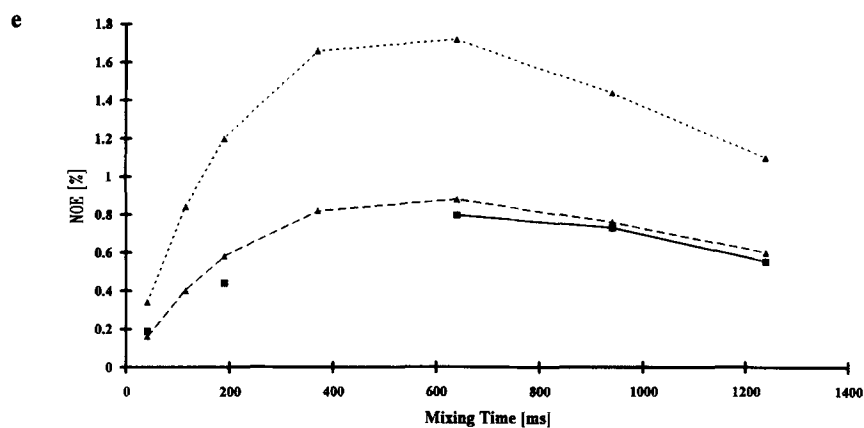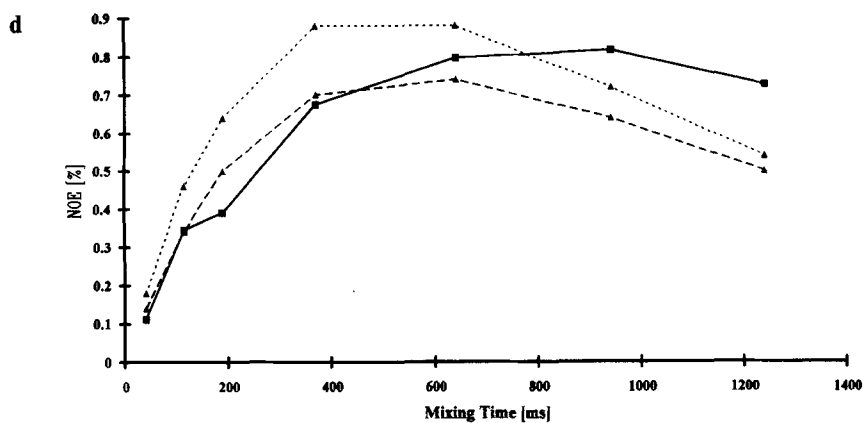
a

b

c

Fig. 5. Experimental and theoretical build-up curves for **1**. For details see experimental part. (a) H1′/H4(H5); (b) H1′/H3; (c) H5′/H4(H5); (d) H5′/H6-*pro*-S; (e) H5′/H6-*pro*-R; (f) H6-*pro*-S/H5′. Experimental curves (square data points):

d

e

f

solid; <NOE>$_{MMC,303\ K}$ (triangle data points): dotted; <NOE>$_{MMC,1000\ K}$ (triangle data points): dashed. In some cases experimental data points are missing (e.g., b). In those cases the neighboring data points are not connected.

were varied. In order to assess the effect of rotation of the hydroxymethyl group on interglycosidic NOEs MMC simulations at 303 K and 1000 K with 10^5 steps each were performed with the α-(1→4) linkage held fixed in conformations A–D. In these simulations ω is the only variable parameter and it is found that all calculated NOEs are almost unaffected by increasing the temperature parameter in these simulations in 1D conformational space (data not shown) because the amount of gt and gg conformers is almost balanced.

The MMC simulations were used to calculate ensemble average $<NOE>_{MMC}$ build-up curves. These theoretical values were compared to the experimental data to estimate the relative population of different parts of conformational space of 1. Also, from experimental coupling constants the amount of gt, gg and tg rotamers was calculated and compared to the corresponding distribution of rotamers resulting from MMC simulations.

DISCUSSION

Experimental and $<NOE>_{MMC}$ build-up curves for the NOEs H1'/H3, H1'/H4(H5), H5'/ H4(H5), H5'/H6-pro-R, H5'/H6-pro-S and H6-pro-S/H5' (Fig. 1) are shown in Fig. 5. In accordance with previous studies it is found that neither the global minimum conformation A nor one of the local minimum conformations B–D can be used as 'single-state models' to satisfactorily account for the NOEs observed (data not shown). Especially, the NOEs H5'/H6-pro-(R)S require at least averaging over conformations at the C5-C6 bond in 1. The MMC simulations where ω was the only variable parameter, clearly indicate that flexibility of the glycosidic linkage also has to be taken into account because none of the minima A–D with the hydroxymethyl group 'rotating' (1D MMC simulations) gives a good fit with the experimental data (data not shown). The MMC-derived ensemble average $<NOEs>_{MMC}$ reproduces the experimental data much better. To estimate the sensitivity of $<NOEs>_{MMC}$ towards differing conformational distributions at the glycosidic linkage in 1, MMC simulations were performed with two temperature parameters, 303 and 1000 K. For the interglycosidic NOE H1'/H4(H5) the fit between experimental and theoretical data is almost independent of the temperature parameter. The situation is different for the 'long-range' NOE between H5' and proton H6-pro-R. Increasing the temperature parameter to 1000 K leads to a significantly improved fit (Fig. 5). Increased temperature parameters generally allow sampling of larger parts of conformational space and surmounting of higher energy barriers between local minima. The improved fit observed is due to widening of the accessible ϕ, ψ-subspace at the (1→4)-glycosidic linkage and not to an increased population of higher energy conformational states at the C5-C6 linkage as will be shown in the following. It can be easily verified via inspection of molecular models that the NOE between H5' and H6-pro-R can occur only if the molecule resides in a conformation close to minima A and B (Fig. 2). If 1 resides in the region of the low-energy island D or in the region of local minimum C the respective proton distances would be too large. Therefore, a higher population of these two regions of conformational space could cause an attenuation of the calculated ensemble average NOE H5'/H6-pro-R leading to the improved fit. Since integration of the conformation distribution for the 1000-K MMC simulation (Fig. 4) yields only 2.5% of all conformations in region D the improved fit must be mainly due to a higher population in the conformational space around minimum C (positive ϕ, ψ values, see Figs. 2 and 4).

MMC simulations where ω is the only variable angle, with temperature parameters set at 303 K

and 1000 K result in almost identical $<NOE>_{MMC}$ build-up curves. This shows that the improved fit between experimental and theoretical build-up curves is not due to an increased amount of higher energy rotamers at the C5-C6 linkage.

The NOE H5′/H4(H5) is rather small but, nevertheless, experimental data for its build-up could be obtained (Fig. 5). It is seen that within the experimental limits the correspondence between experimental and theoretical build-up curves is satisfactory for both settings of the temperature parameter. Since this NOE is rather weak (less than 0.5%) it must be considered less significant than the one observed for the NOE H5′/H6-pro-R.

The NOEs H5′/H4(H5) and H1′/H4(H5) (vide supra) deserve a further comment. No enhancement of H5 would be expected for minima A–C, neither upon selective excitation of H1′ nor of H5′. Only in region D a short distance occurs between H1′ and H5. As a matter of fact, H4 and H5 are strongly coupled and therefore the observed enhancement of H5 (Fig. 1b) does not necessarily indicate a greater amount of conformations residing in region D.

The quality of the experimental data points for the NOE H1′/H3 is not sufficient to allow a quantitative interpretation. However, a comparison of the $<NOE>_{MMC}$ build-up curves with temperature parameters of 303 K and 1000 K shows that this experiment is not sensitive to the value of the temperature parameter (Fig. 5). Nevertheless, the experimental data can be used to estimate an upper limit for the amount of conformations in local minimum D. For conformation D the calculated transient NOE at 0.5 s mixing time is 4.9%, for conformations A, B and C the values are 0.3%, 0.9% and 0.0%, respectively. The experimental build-up curve shows that the maximum experimental enhancement is approximately 1%. Therefore, conformations in region D cannot contribute more than a few percent to the conformational equilibrium in 1. This is in accordance with the MMC simulations. Even with the temperature parameter set at 1000 K, the amount of D-like conformations is only 2.5% (vide supra).

Discrepancies are found between experimental and theoretical values for the intraglycosidic NOEs H5′/CH_3-6′ and H6-pro-R/H6-pro-S (data not shown). In the case of the NOE H5′/CH_3-6′, where the experimental value is twice as high as the calculated one, the three-state jump model was used to describe the internal motion of the methyl group. For an MMC simulation this approximation may be too crude to provide a satisfactory theoretical model. It was tried whether the internal motional correlation time τ_i could influence this NOE but varying τ_i over two orders of magnitude (10^{-13}–10^{-11} s) did not yield significantly different build-up curves. In the case of the NOE H6-pro-R/H6-pro-S, where the experimental value is roughly twice as low as the simulated one, it must be noticed that the distance between the two protons is rather short (ca. 1.9 Å), and, therefore, relatively small variations of bond angles at C6 may cause significant changes of this NOE. Finally, it should be emphasized that effects of anisotropy of motion of 1 have not been taken into account. It is well known that the molecular motion of even small molecules might not be completely isotropic. Also, effects of cross-correlation (Bull, 1987; Krishman and Kumar, 1991), not considered here, may play a role.

From the vicinal coupling constants $J_{5,6}$ (Table 1) the ratio of gg, gt and tg conformers can be calculated. With different parametrizations of the Karplus equation the following ratios were obtained gg:gt:tg=60:40:0 (Gerlt and Youngblood, 1980), gg:gt:tg=71:34:−5 (Streefkerk et al, 1973) and gg:gt:tg=63:52:−15 (Haasnoot et al., 1980). The gg:gt:tg ratio calculated according to Gerlt and Youngblood is closest to the theoretical data obtained above from the MMC simulations.
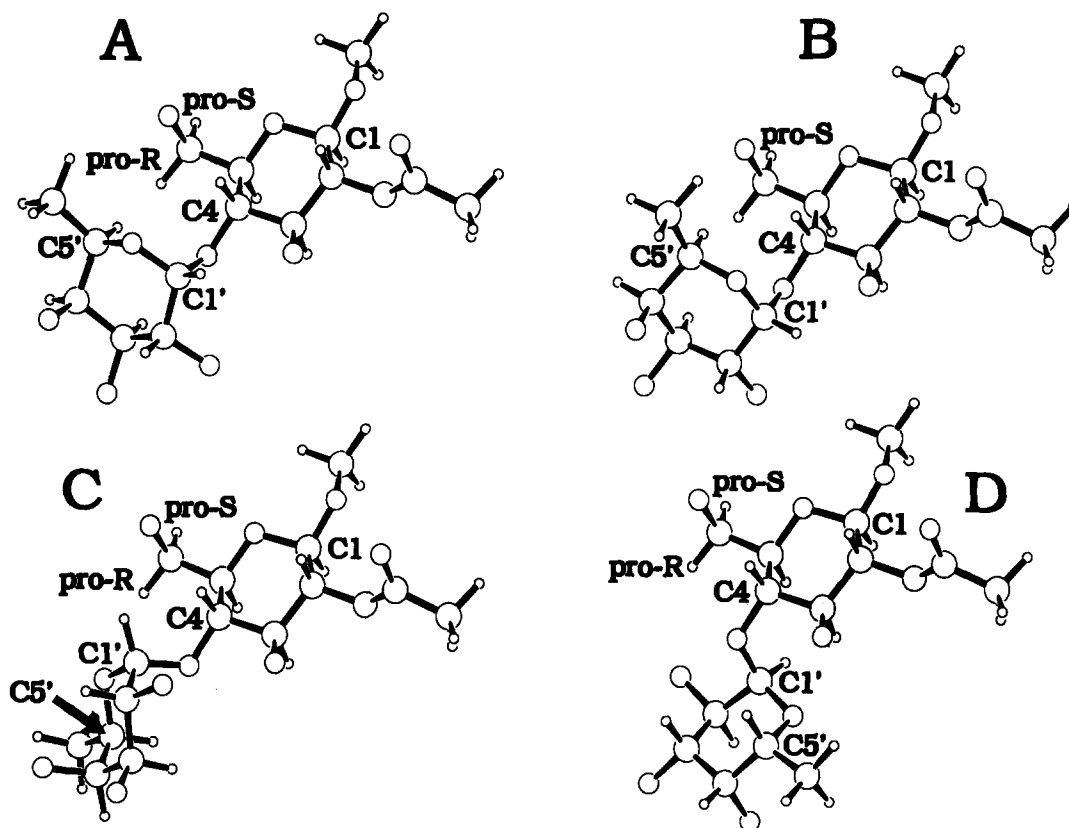
412

Fig. 6. Ball-and-stick models for 1A, B, C and D. Plots were produced with the program SCHAKAL (Keller, E., SCHAKAL-88B, University of Freiburg, 1988).

CONCLUSION

It is shown that the glycosidic linkage in the maltose-related disaccharide 1 must be treated as flexible to account for the experimentally observed NOE build-up curves. This finding is in accordance with previous studies concerning the conformational behavior of maltose (Lemieux and Bock, 1983; Lipkind et al., 1985; Pérez and Vergelati, 1987; Ha et al., 1988; French, 1989; Tran et al., 1989; Peters et al., 1993). In our study, the emphasis was put on the investigation of the dependency of interglycosidic NOEs on conformation distributions at the glycosidic linkage in 1. The temperature parameter was treated as an additional 'artificial' parameter to induce different conformation distributions (Fig. 4). It was found that in 1 only the 'long-range' NOE H5'/H6-*pro*-R shows significant dependence on the conformation distribution. Therefore, this NOE is very useful to more accurately determine the conformation distribution at the α-(1$\rightarrow$4) glycosidic linkage in 1. In the future, it will be important to identify such 'conformation-distribution sensors' for other types of glycosidic linkages.

The use of build-up curves instead of steady-state experiments or measurements at only one mixing time reduces the experimental error because outliers can easily be identified and, addition-

ally, the degree of curvature can be compared to the theoretical data. For 1, which is a low-molecular-weight compound within the positive NOE regime, 1D transient experiments gave the best experimental results for a quantitative analysis. Our study reveals the need of more experimental restraints to define the conformational behavior of saccharides but also the necessity of a rigorous quantitative treatment of interglycosidic NOEs to find those that may serve as 'conformation-distribution sensors'. MMC simulations with different temperature parameters provide a convenient tool to identify these sensors.

On the basis of the experimental build-up curve for the NOE H1'/H3 an upper limit in the range of a few percent could be estimated for the amount of conformer D. This is in accordance with the MMC simulation at 1000 K which predicted ca. 2.5% of all conformers residing in the low-energy island around D (Figs. 1 and 6). From a comparison of experimental with calculated NOE build-up curves it could also be concluded that conformations with positive ϕ and ψ angles (region C, Figs. 1 and 6) should contribute significantly to the conformational equilibrium at the α-(1→4) linkage in 1. To visualize the conformational flexibility of 1 Fig. 6 shows ball-and-stick models for the minima A, B, C and D.

ACKNOWLEDGEMENTS

REFERENCES

Anders, U. (1989) Ph.D. Thesis, University of Frankfurt.
Bock, K. (1983) *Pure Appl. Chem.,* **55,** 605–622.
Bock, K., Lönn, H. and Peters, T. (1990) *Carbohydr. Res.,* **198,** 375–380.
Boelens, R., Koning, T.M.G., van der Marel, G.A., van Boom, J.H. and Kaptein, R. (1989) *J. Magn. Reson.,* **82,** 290–308.
Borgias, B.A. and James, T.L. (1989) *Methods Enzymol.,* **176,** 169–184.
Brisson, J.-R. and Carver, J.P. (1983) *Biochemistry,* **22,** 1362–1368.
Bull, T.E. (1987) *J. Magn. Reson.,* **72,** 397–413.
Cook, W.J. and Bugg, C.E. (1975) *Biochem. Biophys. Acta,* **389,** 428–435.
Cumming, D.A. and Carver, J.P. (1987a) *Biochemistry,* **26,** 6664–6676.
Cumming, D.A. and Carver, J.P. (1987b) *Biochemistry,* **26,** 6676–6683.
Dejter-Juszynski, M. and Flowers, H.M. (1971) *Carbohydr. Res.,* **18,** 219–226.
French, A.D. (1989) *Carbohydr. Res.,* **188,** 206–211.
Gerlt, J.A. and Youngblood, A.V. (1980) *J. Am. Chem. Soc.,* **102,** 7433–7438.
Ha, S.N., Madsen, L.J. and Brady, J.W. (1988) *Biopolymers,* **27,** 1927–1952.
Haasnoot, C.A.G., De Leeuw, F.A.A.M. and Altona, C. (1980) *Tetrahedron,* **36,** 2783–2792.
Heatley, F., Akhter, L. and Brown, R.T. (1980) *J. Chem. Soc., Perkin Trans. 2,* 919–924.
Homans, S.W. (1990) *Biochemistry,* **29,** 9110–9118.
Imberty, A., Tran, V. and Pérez, S. (1989) *J. Comput. Chem.,* **11,** 205–216.
Kay, L.E., Scarsdale, J.N., Hare, D.R. and Prestegard, J.H. (1986) *J. Magn. Reson.,* **68,** 515–525.
Kessler, H., Oschkinat, H. and Griesinger, C. (1986) *J. Magn. Reson.,* **70,** 106–133.
Kessler, H., Mronga, S. and Gemmecker, G. (1991) *Magn. Reson. Chem.,* **29,** 527–557.

414

Krishnan, V.V. and Kumar, A. (1991) *J. Magn. Reson.,* **92,** 293–311.

Lemieux, R.U. and Bock, K. (1983) *Arch. Biochem. Biophys.,* **221,** 125–134.

Lipkind, G.M., Shashkov, A.S. and Kochetkov, N.K. (1985) *Carbohydr. Res.,* **141,** 191–197.

Marion, D. and Wüthrich, K. (1983) *Biochem. Biophys. Res. Commun.,* **113,** 967–974.

Meyer, B. (1990) *Topics Curr. Chem.,* **154,** 141–208.

Neuhaus, D. and Williamson, M. (1989) *The Nuclear Overhauser Effect in Structural and Conformational Analysis,* VCH Publishers, Inc., New York, pp. 123–135.

Nishida, Y., Hori, H., Ohrui, H., Meguro, H., Uzawa, J., Reimer, D., Sinnwell, V. and Paulsen, H. (1988) *Tetrahedron Lett.,* **29,** 4461–4464.

Noggle, J.H. and Schirmer, R.E. (1971) *The Nuclear Overhauser Effect,* Academic Press, New York.

Ohrui, H., Nishida, Y., Watanabe, M., Hori, H. and Meguro, H. (1985) *Tetrahedron Lett.,* **26,** 3251–3254.

Pérez, S. and Vergelati, C. (1977) *Polym. Bull,* **17,** 141–148.

Peters, T., Brisson, J.-R. and Bundle, D.R. (1990) *Can. J. Chem.,* **68,** 979–988.

Peters, T., Meyer, B., Stuike-Prill, R., Somorjai, R. and Brisson, J.-R. (1993) *Carbohydr. Res.,* **238,** 49–73.

Peters, T. and Weimar, T. (1991) *Liebigs Ann. Chem.,* 237–242.

Poppe, L. and van Halbeek, H. (1991a) *J. Am. Chem. Soc.,* **113,** 363–365.

Poppe, L. and van Halbeek, H. (1991b) *J. Magn. Reson.,* **93,** 214–217.

Poppe, L., Stuike-Prill, R., Meyer, B. and van Halbeek, H. (1992) *J. Biomol. NMR,* **2,** 109–136.

Press, W.H., Flannery, B.P., Teukolsky, S.A. and Vetterling, W.T. (1986) *Numerical Recipes,* Cambridge University Press, Cambridge, p. 523ff.

Rowan III, R. and Sykes, B.D. (1975) *J. Am. Chem. Soc.,* **97,** 1023–1027.

Streefkerk, D.G., de Bie, M.J.A. and Vliegenthart, J.F.G. (1973) *Tetrahedron,* **29,** 833–844.

Stuike-Prill, R. and Meyer, B. (1990) *Eur. J. Biochem.,* **194,** 903–919.

Stuike-Prill, R. and Meyer, B. (1993) *Can. J. Chem.,* submitted.

Thøgersen, H., Lemieux, R.U., Bock, K. and Meyer, B. (1982) *Can. J. Chem.,* **60,** 44–57.

Tran, V., Buleon, A., Imberty, A. and Pérez, S. (1989) *Biopolymers,* **28,** 679–690.

Vold, R.L., Waugh, J.S., Klein, M.P. and Phelps, D.E. (1968) *J. Chem. Phys.,* **48,** 3831–3832.

Widmalm, G., Byrd, R.A. and Egan, W. (1992) *Carbohydr. Res.,* **229,** 195–211.

Williamson, M. and Neuhaus, D. (1987) *J. Magn. Reson.,* **72,** 369–375.

Winter, W.T., Arnott, S., Isaac, D.H. and Atkins, E.D.T. (1978) *J. Mol. Biol.,* **125,** 1–19.